High-voltage multichannel rail gap switch triggered by corona discharges

Jorge Niedbalski[a)]
Consejo Nacional de Investigaciones Científicas y Técnicas (CONICET), Centro de Investigaciones en Láseres y Aplicaciones CEILAP (CITEFA–CONICET), Juan Bautista de La Salle 4397, (B1603ALO) Villa Martelli, Buenos Aires, Argentina

(Received 30 October 2002; accepted 28 April 2003)

A simple trigger assembly designed to promote multichannel breakdown in a high-voltage low-inductance rail gap switch operating in a dc voltage hold-off mode is described. The switch is formed by two extended (rail) cylindrical electrodes, separated by spacing of 10 mm and pressurized with nitrogen or air up to about 0.5 bar. The gas breakdown in multiple sites of the interelectrode volume is initiated by preionization with ultraviolet radiation pulses simultaneously emitted from an array of circular orifices and is performed along one generatrix of the surface of a tabular electrode (cathode) which are generated in its interior by capacitively coupled (pulsed corona) discharges. The switch has been tested by discharging capacitors of 40 and 100 nF in an underdamped condition at voltages and peak currents up to 15 kV and 14 kA, respectively. The maximum energy transferred per shot was about 11 J. The trigger assembly allows one to arbitrarily select the number of channels to be formed just by varying the number of preionization sources (orifices) distributed in the cathode and as a result they are unaffected by the discharges.
[DOI: 10.1063/1.1584081]

I. INTRODUCTION

The feasibility of scaling in power levels to be transferred from high-capacity banks on high-voltage pulsed discharge circuits,[1] currently employed for laser pumping application of them, is mainly conditioned by high-voltage switches through the damage caused by erosion at their discharge electrodes. This damage becomes extremely severe in the case of conventional spark gaps (trigatron type) when high power is transferred because of localization of the discharges within a relatively small area of both electrodes. For working conditions in which high current peaks, fast switching, and long lifetime electrodes are necessary a rail gap switch that operates through a large number of simultaneous breakdown channels distributed along their electrodes constitutes the simplest and most efficient device to satisfy these requirements.

For many years, low-inductance rail gap switches used in combination with low-impedance pulse-forming lines (PFLs) have been of particular interest in excimer laser technology to produce short rise time excitation pulses.[2,3] A variety of switches containing different trigger assemblies and discharge electrodes with uniform and highly nonuniform (knife-edge) profiles were developed for that application.[4–6] Most of the trigger assemblies proposed are based on gas photopreionization produced by both incoherent and coherent ultraviolet (UV) radiation provided by sparks,[4,5] corona discharges,[4,5] rare-gas halide (KrF) lasers,[5] and semiconductor edge discharges.[6] Each of these devices is typically operated under a dynamic condition by synchronizing triggering of the radiation at the instant at which its interelectrode gap is highly overvolted compared to its corresponding dc self-breakdown voltage. This operating characteristic facilitates multichannel performance considerably. In fact, the large spatial, temporal electric field gradients that appear between switch electrodes during the relatively fast charging procedure of the PFL minimize the demand that preionization levels be generated by irradiation to initiate the gas breakdown process. In contrast, multichannel performance is very much more difficult to obtain when both electric field gradients are totally removed, i.e., when the switch must operate in a dc voltage hold-off mode and uniform field electrodes must also be employed for a potentially long lifetime. In this case, the role of the trigger assembly becomes crucial because of the necessity of generating very high photoelectron densities in the gas to compensate for the initially static, somewhat reduced interelectrode electric field.

In this work, a simple trigger assembly based on capacitively coupled (pulsed corona) discharges as UV radiation sources is used to promote multichannel breakdown in a scalable high-voltage rail gap switch operating in dc voltage hold-off mode. The assembly basically differs from those reported in Refs. 4 and 5 in that the corona discharge takes place in the interior of one of the discharge electrodes (a tubular electrode), with the gas irradiated through an array of orifices linearly distributed along its surface. Advantageous features introduced by this assembly are (a) optimal adaptation (by its very close proximity) to the main discharge region, which provides efficient UV radiation-pressurization gas coupling and (b) overall control of the number of channels to be formed and of its distribution along the electrodes.

II. RAIL GAP DESIGN

A cross-sectional view of the device is shown in Fig. 1. The discharge electrode is a hemicylindrical brass rod (high-

a)Electronic mail: jniels@infovia.com.ar

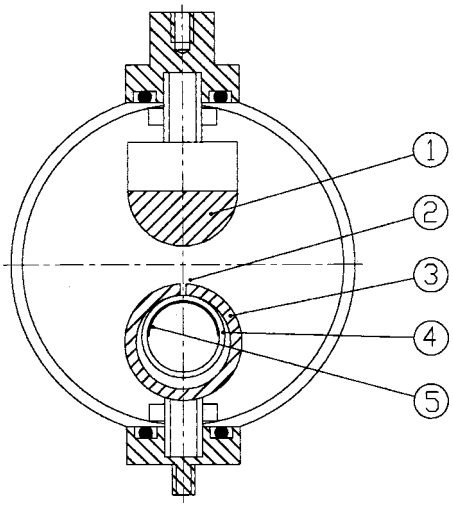

FIG. 1. Cross-sectional view of the rail gap switch and corona trigger assembly. (1) High-voltage electrode; (2) orifice (diameter 1.5 mm); (3) tubular electrode (cathode); (4) borosilicate glass tube (thickness 1.5 mm); (5) copper foil (thickness 100 μm).

voltage electrode) of 0.9 cm radius, 15 cm long and a tube of the same material with 1.3 cm inner diameter (i.d.), 1.9 cm outer diameter (o.d.), 17.5 cm long which is connected at ground potential. Both ends of the high-voltage electrode were conveniently contoured to minimize geometrical intensification of the electric field in the interelectrode region. Ten orifices 1.5 mm in diameter, separated by spacing of 10 mm, were made along one generatrix of the tubular electrode surface; small burrs produced by the wick located at their periphery were removed by mechanical rectification of the inner surface of the tube. The corona trigger assembly (CTA) which featured a dielectric tube of 7 mm i.d., 10 mm o.d., 21 cm long inside which a thin (100-μm-thick) copper foil, previously welded to a high-voltage cable which serves as an external connection to the trigger generator, was adjusted along its length to the wall. At the same time, this arrangement was introduced into the tubular electrode and uniformly pressed against the region containing the orifice distribution. The electrodes were housed in a transparent Lucite cell which allowed pressurization with nitrogen or air up to about 1.2 bar and modification of the interelectrode separation up

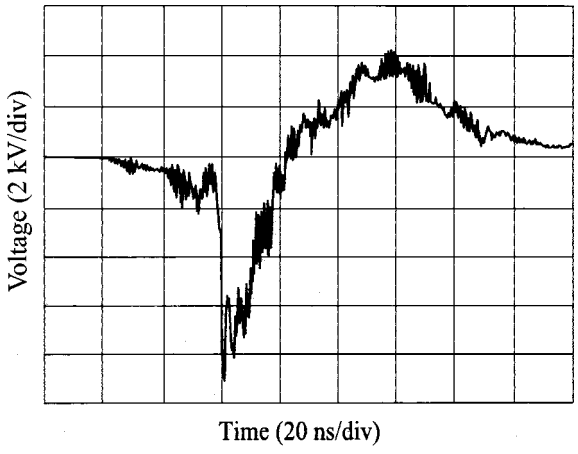

FIG. 2. High-voltage pulse applied to the corona trigger assembly.

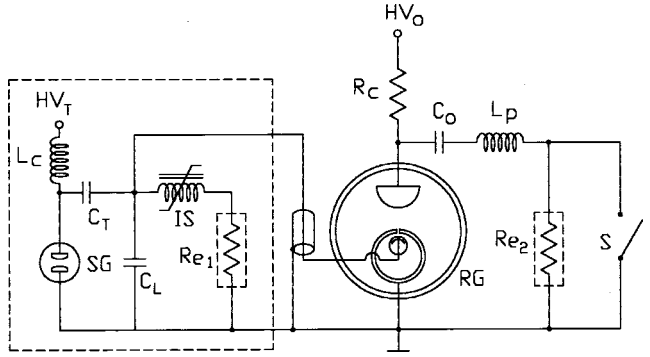

FIG. 3. Schematic diagram of the rail gap test circuit and subcircuit of the trigger generator (inside the area delineated by the dashed trace). SG=low-inductance (3 nH) spark gap; C_T=1 nF; C_L≈4 pF; IS=saturable inductor; Re_1≈100 Ω (electrolitic resistor); RG=rail gap switch; R_c=1 MΩ; C_0 =40 or 100 nF; L_p parasitic inductance; Re_2≈4 Ω (electrolitic resistor).

to 13 mm. The rail gap structural inductance, estimated as one-half of a single-turn solenoide,[7] was about 12 nH. Reduction of this value could be achieved by increasing the length of the discharge electrode.

The CTA was excited with high-voltage negative pulses with about 2 ns rise time and 16 ns duration [full width at half maximum (FWHM)], as shown in Fig. 2, which is provided by a small generator based in a capacitive discharge on a coaxial choke line loaded with toroidal cores of saturable magnetic material.[8]

III. OPERATING CHARACTERISTICS

Figure 3 illustrates a schematic diagram of the circuit employed for testing the performance of the rail gap switch; shown inside the area delineated by the dashed trace is the subcircuit that corresponds to the trigger generator. Capacitors (C_0) of 40 and 100 nF were discharged separately either in an overdamped condition using $CuSO_4$ electrolitic resistors (Re_2) as the dissipation load or in an underdamped condition with the rail gap itself being the main load (Re_2 shorted). The parasitic inductance L_p of the circuits esti-

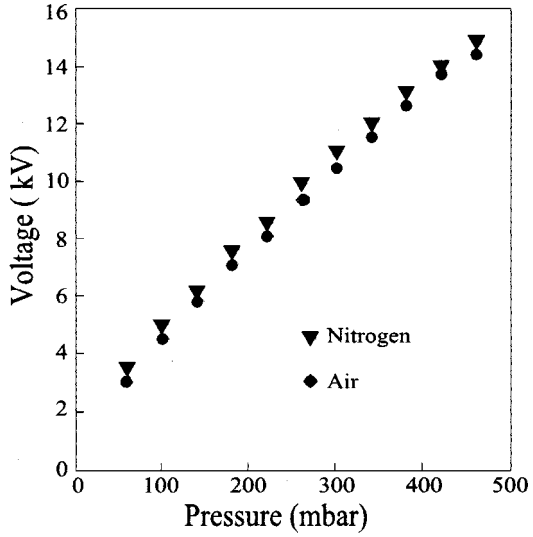

FIG. 4. Self-breakdown voltage of the rail gap switch as a function of the gas pressure for an interelectrode gap separation of 10 mm.

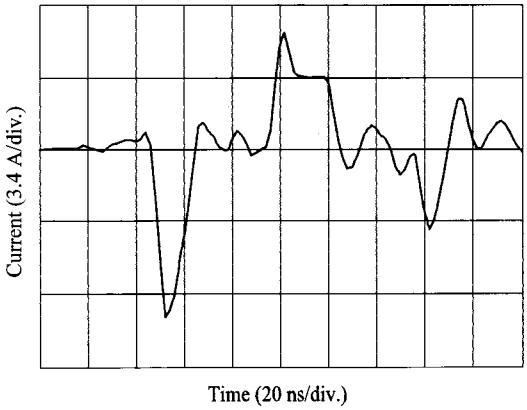

FIG. 5. Temporal evolution of the current associated with corona discharge.

mated from the voltage oscillation frequencies when the rail gap undergoes self-breakdown through a single discharge channel were 77.6 and 91 nH, respectively.

In operation, C_0 is dc charged at a working voltage V_0 close to the self-breakdown threshold V_{bd} of the switch determined by the interelectrode gap spacing (d), cell pressure (p), and filling gas type involved, and subsequently triggered by applying the excitation pulse to the CTA. Throughout this work d was set at 10 mm whereas p was varied up to a maximum of about 0.5 bar. Figure 4 shows V_{bd} as a function of p for nitrogen and air obtained by discharging the 40 nF capacitor.

There are two critical requirements that ought to be satisfied in conjunction with the CTA and the excitation pulse for a given pressurization gas (N_2 or air) in order to promote multichannel breakdown. First is to generate radiation pulses with sufficient intensity and with photon energies $h\nu \geqslant 14.5$ eV (the nitrogen ionization energy) to produce within the gas, via absorption of a single photon, the necessary photoelectron density for each value of the interelectrode electric field (V_0/pd) to initiate the breakdown process. Second is to simultaneously provide similar preionization levels in the immediate neighborhood of each source (orifice) to distribute the discharge current equally between channels. Due to the fast loss of free electrons, which predominantly takes place via electron–ion recombination immediately after the onset of irradiation, the photoelectron density (so much in nitrogen as in air) can only be maintained at a relatively high level for

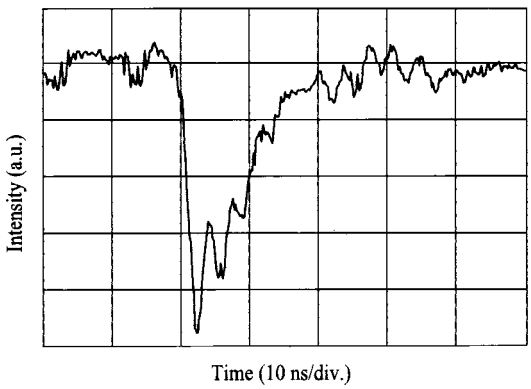

FIG. 6. Temporal evolution of the radiation pulse emitted by the corona discharge from an orifice.

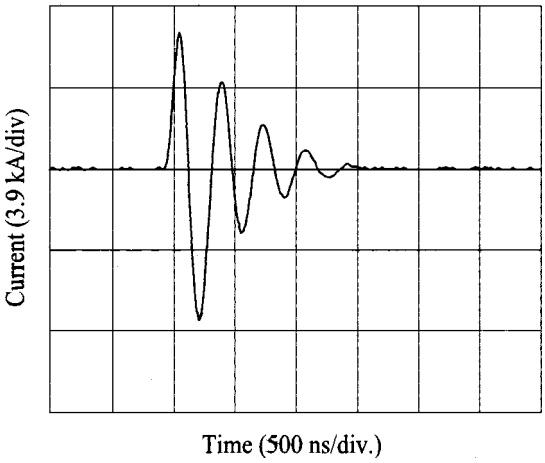

FIG. 7. Oscillogram of the circuit current obtained by switching the 40 nF capacitor through a single breakdown channel for charge voltage $V_0 = 10$ kV with Re_2 shorted.

a short period of time (a few ns). This imposes an additional requirement upon the temporal shape of the radiation pulses to be generated, which might have as a particular feature a rise time of the same order of the magnitude or less than the electron–ion recombination time.

Available tubes of various types of glass (borosilicates) all of which had relatively low permittivity ($\varepsilon_r \approx 4-6$) were tested in the CTA. Fortunately, the structure of these materials has attractive physical properties for the present application, such as negligible variation of the permittivity within a wide frequency range and linear behavior (in the absence of hysteresis effects), as a response to the main Fourier frequency component (500 MHz) associated with the excitation pulse rise time (2 ns). By using small probe disks of similar types of glass, the dielectric properties mentioned were experimentally verified at low voltage in the frequency range of 100–600 MHz by means of a HP 4291A impedance-material analyzer.

The application of the excitation pulse to the CTA produces diffuse corona discharges which appear synchronously in all orifices confined to the interstitial region limited by their contours in contact with the glass tube surface. Each

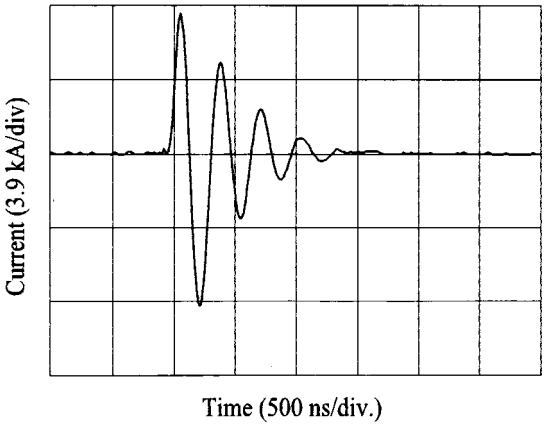

FIG. 8. Oscillogram of the circuit current obtained by switching the 40 nF capacitor through nine breakdown channels for charge voltage $V_0 = 10$ kV with Re_2 shorted.

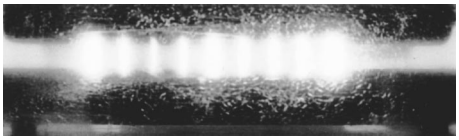

FIG. 9. Photograph of an open shutter of switch breakdown taken during discharge of the 100 nF capacitor with Re_2 shorted. The charge voltage and discharge current peak were 10 kV and about 10 kA, respectively.

individual discharge develops within a highly magnified electric field introduced by the abrupt profile of the orifice contour, with associated current that typically contains very energetic electrons. Therefore, according to Ref. 9, hard UV radiation emission is expected. Note, however, that the reduced CTA capacitance due particularly to both the low ε_r value and the relatively large thickness of the glass tube (1.5 mm) limit the amplitude of the corona current[10] and consequently the intensity of the UV radiation pulses at relatively low levels for acceptable excitation voltages (normally varied up to the 10 kV peak in the present work).

Figure 5 shows the temporal evolution of the corona current monitored by a Rogowski coil and displayed on a digital oscilloscope (HP 54510 A). A typical radiation pulse emitted from an orifice, detected by a fast photomultiplier (S-5 photodiode surface, 200 ps rise time) is shown in Fig. 6. Fluctuations of amplitude in consecutive shots were in both cases within of $\pm 10\%$. Linear correspondence between the excitation and radiation pulse amplitudes was verified.

On the basis of shot to shot operation, multichannel switch performance was found to be strongly dependent on voltage V_0 with respect to V_{bd} within the entire range of pressure (Fig. 4); in every instance the best result obtained was for $V_0/V_{hd} \approx 0.95-0.98$. The parallel between electrodes resulted in also being a critical factor; for reliable multichannel performance it was typically adjusted to within 30 mrad. Both circuits were operated up to a maximum charge voltage of 15 kV, corresponding to a switch working pressure of about 470 mbar. At higher pressures, a gradual trend toward a reduction of the number of channels was observed. The maximum energy transferred by a shot was about 11 J, which in great part dissipated in the switch itself.

Figures 7 and 8 show characteristic oscillograms of the circuit currents obtained by switching the 40 nF capacitor in the underdamped condition (Re_2 shorted) through channels one and nine, respectively, which had identical discharge parameters ($V_0 = 10$ kV, $p \approx 270$ mbar). As a function of the energy to be transferred the number of operating channels could arbitrarily be either reduced by inhibiting the gas irradiation from the CTA, for instance, indistinctly sealing some orifices, or increased by making additional orifices.

From a comparison between the wave forms in Figs. 7 and 8, it should be noted how the oscillation frequency and the amplitude become slightly increased as the number of breakdown channels increases. This result is attributed physically to the effect of the proper switch on the circuit through the inductive and resistive components, respectively, associated with its closure discharge.[5]

The photograph of the open shutter shown in Fig. 9 illustrates an example of multichannel switch performance. The photograph was taken during switching of the 100 nF capacitor in the underdamped condition for $V_0 = 10$ kV; the discharge current of the 10 kA peak was shared in nine channels, each carrying a small fraction of the same. In consecutive shots the current wave form was reproduced well. The delay between the excitation pulse applied to the CTA and the switch closure current was about 160 ns. Inspection of the CTA after several hundred shots did not show any visible signs of damage.

Improvement in the switch capability to extend multichannel performance at pressures higher than 0.5 bar and therefore at higher working voltages can certainly be achieved by a substantial increase in UV radiation intensity generated by the CTA, for instance, by replacing the glass tube by a ceramic tube. Because of its very high permittivity value ($\varepsilon_r \sim 13\,000$) and relatively high dielectric strength, a possible candidate appears to be bariumtitanate bariumstanate. This material, employed to manufacture the discharge electrodes of a millimeter dimension high-pressure (1 bar) N_2 laser, showed linear behavior in its temporal response to relatively fast high-voltage excitation pulses (1 ns rise time).[11]

[1] H. Houtman, A. Cheuck, A. Elezzabi, J. Ford, M. Laberge, W. Liese, J. Meyer, G. Stuart, and Y. Zhu, Rev. Sci. Instrum. **64**, 839 (1994).
[2] M. Osborne, P. Smith, and M. Hutchinson, Opt. Commun. **52**, 415 (1985).
[3] R. Taylor, P. Corkum, S. Watanabe, K. Leopold, and A. Alcock, IEEE J. Quantum Electron. **19**, 416 (1983).
[4] D. Cohn, W. Long, E. Stappaerst, M. Plummer, and J. West, Rev. Sci. Instrum. **53**, 253 (1982).
[5] R. S. Taylor and K. E. Leopold, Rev. Sci. Instrum. **56**, 52 (1984).
[6] N. Seddon and P. H. Dickinson, Rev. Sci. Instrum. **58**, 804 (1987).
[7] D. Halliday and R. Resnick, *Physics* (Wiley, New York, 1966).
[8] N. Seddon and E. Thornton, Rev. Sci. Instrum. **59**, 2497 (1988).
[9] R. Marchetti, E. Penco, E. Armandillo, and G. Salvetti, J. Appl. Phys. **54**, 5672 (1983).
[10] R. Gratton, S. Mangioni, and J. Niedbalski, J. Phys. D **24**, 11 (1991).
[11] V. Hasson, H. von Bergmann, and E. Jones, Rev. Sci. Instrum. **51**, 384 (1980).